

**OPEN ACCESS**

## Structural effects of niobium and silver doping on titanium dioxide nanoparticles

To cite this article: A Ahmad *et al* 2007 *J. Phys.: Conf. Ser.* **61** 11

View the [article online](#) for updates and enhancements.

### You may also like

- [Fe–Y–M–B \(M = Nb or Ta\) bulk metallic glasses with ultrahigh strength and good soft magnetic properties](#)  
Chih-Yuan Lin, Mou-Cheng Lee and Tsung-Shune Chin
- [Influence of Niobium and Zirconium Alloying Additions on the Anodic Dissolution Behavior of Activated Titanium in HCl Solutions](#)  
Steven Y. Yu, John R. Scully and Carrisima M. Vitus
- [Effects of Nb and Mo additions on thermal behavior, microstructure and magnetic property of FeCoZrBGe alloy](#)  
Yaming Sun, , Zhiqun Wang et al.



**ECS**  
The  
Electrochemical  
Society  
Advancing solid state &  
electrochemical science & technology

**DISCOVER**  
how sustainability  
intersects with  
electrochemistry & solid  
state science research

## Structural effects of niobium and silver doping on titanium dioxide nanoparticles

A. Ahmad<sup>1</sup>, J. Thiel<sup>2</sup>, and S. Ismat Shah<sup>2</sup>

<sup>1</sup>Department of Metallurgical and Materials Engineering  
University of Engineering and Technology, Lahore, Pakistan

<sup>2</sup>Department of Materials Science and Engineering  
University of Delaware, Newark, DE 19716

E.mail: [aamalik87@fulbrightweb.org](mailto:aamalik87@fulbrightweb.org)

**Abstract.** Pure, Nb-doped and Ag-doped titania nanoparticles were synthesized by sol-gel technique with dopant concentrations ranging from 0.5 to 1.5 atomic percent Nb or Ag. The annealing temperatures ranged from 250 to 900 °C. Changes in phase transformation of the doped samples with reference to pure titania were studied. It was found that Nb doping stabilizes the anatase phase while Ag doping accelerates the transformation from anatase to rutile at a concentration higher than 0.5 at. %. The samples were analyzed by X-ray diffraction (XRD), Scanning Electron Microscopy (SEM), Transmission Electron Microscopy (TEM), X-ray Photoelectron Spectroscopy (XPS) and Energy Dispersive X-ray Spectroscopy (EDS).

### 1. Introduction

The band gap (E<sub>g</sub>) of TiO<sub>2</sub> anatase is ~3.2eV [1] and lies in the UV range so that only 5-8 % of sunlight photons have the required energy to activate the catalyst. This relatively large band gap has significantly limited application, particularly in indoor situations. An effective way to improve the TiO<sub>2</sub> photocatalytic activity is to introduce foreign metal ions as dopants into its lattice. Depending on the dopant type and concentration, the band gap of TiO<sub>2</sub> can be tailored to extend the photoresponsiveness into the visible light region. Among the various methods used for the synthesis of titania nanoparticles the sol-gel process is a most attractive method to introduce foreign metal ions into TiO<sub>2</sub> powders and films [2,3]. One of the problems in both catalytic and sensor applications of anatase based material is its transformation to rutile. This transformation is dependent on several parameters such as initial particle size, initial phase, dopant concentration, reaction atmosphere and annealing temperature etc [2,4].

The dopants introduced by sol-gel method usually affect the TiO<sub>2</sub> phase transformation behavior and structure. It is therefore interesting and necessary to examine the effect of dopants on the TiO<sub>2</sub> phase transformation and grain growth before their application.

The interest in Nb-doped TiO<sub>2</sub> derives from the fact that Nb doping leads to enhanced photocatalytic activity in the destruction of many organic pollutants [5]. Antibacterial titanium dioxide doped with silver finds applications in aerospace, for coating of surfaces in refrigerators, on kitchen furniture or in hospitals. Research indicates that it is also effective in purification systems for disinfecting water or air [6]. In this paper we describe the synthesis of TiO<sub>2</sub> nano particles by sol gel

method doped with Nb or silver. The effect of Nb and Ag ion doping on the phase transformation of anatase to rutile crystal structure is discussed in detail.

## 2. Experimental

Sol-gel technique was used to synthesize pure, Nb-doped and Ag-doped titania nanoparticle. Titanium tetrachloride was used as  $\text{TiO}_2$  precursor. For Nb-doped  $\text{TiO}_2$  nano particles niobium penta-ethoxide  $\text{Nb}(\text{OC}_2\text{H}_5)_5$  was used as Nb precursor. For Ag-doped samples silver acetylacetonate  $\text{Ag}(\text{CH}_3\text{COCHCOCH}_3)_3$  was used as Ag precursor.

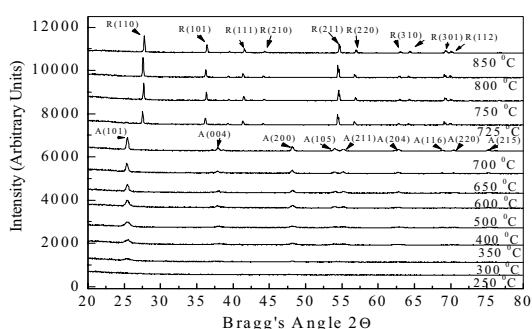
The doped titania nanoparticles containing 0.5 to 1.5 atomic % Nb or Ag were synthesized. The dopant stoichiometry was controlled by dissolving the Nb or Ag precursors in ethanol (Pharmco 200 proof) prior to the drop wise addition of  $\text{TiCl}_4$ . The reaction was performed at room temperature while stirring under a fume hood due to the large amount of  $\text{Cl}_2$  and HCl gases evolved in this reaction. The resulting yellow solution was allowed to rest and cool to room temperature as the gas evolution ceased. The suspensions obtained were dried in an oven for several hours at 60-80 °C until dried  $\text{TiO}_2$  particles were obtained. The as-synthesized Nb and Ag doped samples were calcined for one hour in a box furnace at temperature ranging from 300 to 850 °C in an ambient atmosphere. X-ray diffraction (XRD) analysis of doped and undoped  $\text{TiO}_2$  powders was carried out on a Rigaku D-Max B diffractometer equipped with a graphite crystal monochromator, operating with a Cu anode and a sealed X-ray tube. The  $2\theta$  scans were recorded at several resolutions using Cu  $K_\alpha$  radiation of wavelength 1.54 Å in the range 20-80° with 0.05° step size. The recorded patterns were analyzed using Jade® software to determine peak position, width and intensity. Full-width at half-maxima (FWHM) data was analyzed by Scherer's formula to determine average particle size. Measurements of particle size and distribution were also carried out by TEM. Both bright field and dark field micrographs were taken with a JEOL JEM-2000FX operating at 200 kV.

The dopant concentration was verified by energy dispersive x-ray spectroscopy (EDS) and XPS. XPS was also employed to characterize the oxidation state of the Nb in Nb-doped samples. Peak positions were internally referenced to the  $\text{C}_{1s}$  peak at 284.6 eV. The Ti 2p, Nb 3d and Ag 2p regions were used to measure the composition of the nanoparticles and to ascertain the valence states of Ti and the dopants.

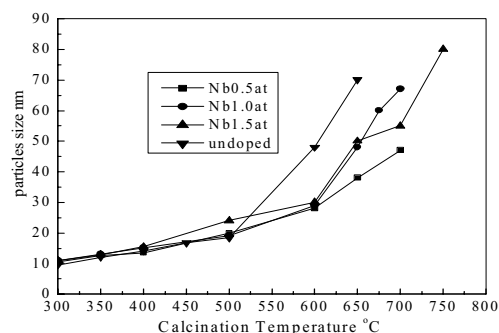
## 3. Results and Discussion

Figure 1 shows the XRD patterns obtained for 0.5 at % Nb doped  $\text{TiO}_2$  sample calcined at various temperatures. The figure shows that particles calcined up to 250 °C were amorphous. Transformation to anatase with presence of large amorphous band in x-ray spectrum is evident at 300 °C. The first XRD peaks to appear were all anatase. As the annealing temperatures increased, the anatase peaks became stronger and sharper indicating improved crystallinity. Pure anatase persisted up to 700 °C. The anatase peaks were indexed as (101), (004), (200), (105), (211), (204), (116), (220) and (215) in the order of increasing diffraction angles, indicating a body centered tetragonal crystalline structure of  $\text{TiO}_2$  crystal. Peaks were broad at low calcination temperatures indicating small  $\text{TiO}_2$  nanocrystalline particle size. Calcination at 725 °C induced a sharp phase transition from anatase to rutile. No anatase related peaks were observed at or above 750 °C indicating the complete phase transformation from anatase to rutile. From the XRD data of Figure1, it is evident that the crystallite size increased with increasing calcinations temperature and that the diffraction peaks became intense and their FWHM gradually became narrow suggesting an increase in particles size and increase in the amount of the pertinent phase. The anatase (101) peak was used to determine the grain size by Scherer's formula. The results of the grain size analysis of undoped and Nb-doped samples are presented in Figure 2. As evident from the Figure the grain growth for the undoped sample at temperatures above 500 °C is higher than the samples doped with Nb.

Figures 3a and 3b show the XRD patterns of 0.5 at %, 1 at % and 1.5 at % Nb doped samples



**Figure 1.** X-ray diffraction patterns as a function of calcination temperature for 0.5 atomic % Nb(v)-doped nanostructured titania (A, anatase;R, rutile)



**Figure 2.** Particles size of undoped and Nb- doped  $\text{TiO}_2$

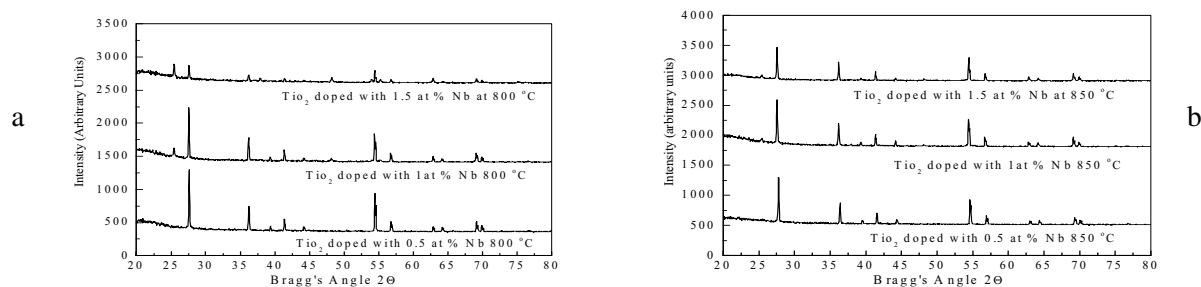


**Figure 3.** X-ray diffraction patterns of Nb-doped titania calcined at (a) 800 °C (b) 850 °C

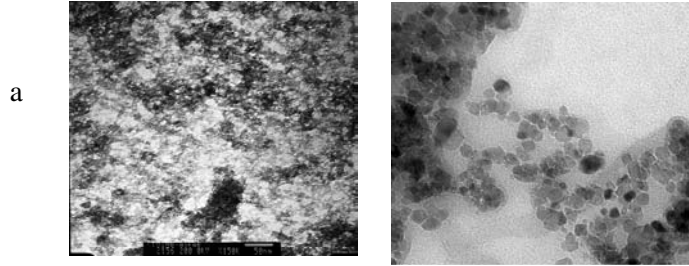
calcined at, 800 °C and 850 °C respectively. It is evident that both the Nb content and calcinations temperatures influenced the percentage of anatase and rutile phases present in the samples. Increasing the Nb content in the doped samples has stabilized the anatase phase. For samples doped with 1 at % and 1.5 at % Nb the transformation from anatase to rutile is not as steep as it happens in 0.5 at % Nb doped samples. As evident from their XRD patterns a mixture of anatase and rutile phase is present up to 850 °C and complete transformation to rutile phase occurred above 850 °C for both samples.

Our results are consistent with the results of Arbiol et al [7] who studied the effect of Nb doping in samples synthesized by induced laser pyrolysis. They found that presence of Nb substitutional ions in the anatase structure hinders the particles growth and transformation from anatase to rutile in  $\text{TiO}_2$  nano particles. The atomic radii of  $\text{Nb}^{+5}$  is 0.70 Å while that of  $\text{Ti}^{+4}$  is 0.68 Å. This similarity of atomic radii suggest that solubility of Nb in  $\text{TiO}_2$  phases will depend mainly on the charge compensation mechanism rather than on the induced stress. As proposed by Arbiol et al [7], the introduction of Nb should reduce the amount of oxygen vacancies due to it having a higher positive charge than Ti. When Nb ions enter substitutionally into  $\text{TiO}_2$  the charge of  $\text{Nb}^{+5}$  ions should be compensated for a decrease in oxygen vacancies, leading to the hindering of the anatase to rutile transformation.

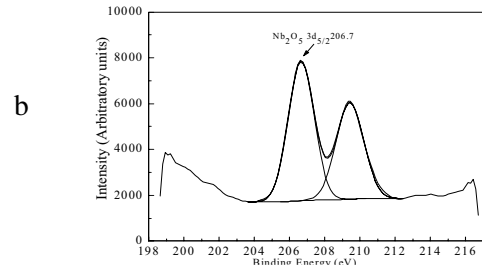
The particle size of doped  $\text{TiO}_2$  was also analyzed by TEM. Figures 4a and 4b show the TEM bright field images of  $\text{TiO}_2$  doped with 0.5 at % Nb as synthesized and calcined at 500 °C, respectively. The particles size measured by TEM were generally in agreement with those determined by XRD though some agglomeration is present due to high surface energy of the particles.

Figure 5 shows high-resolution XPS spectra of the Nb 3d region of the  $\text{TiO}_2$  sample doped with 1 at % Nb. Metallic Nb 3d<sub>5/2</sub> and 3d<sub>3/2</sub> peaks occur at 202 and 205 eV, respectively. No such peaks were observed in the doped sample. Therefore, there is no evidence to suggest the presence of Nb metal clusters within the detection limit of XPS which is dependent on the concentration (approximately 500 ppm) escape depth of the Nb 3d photoelectrons (approximately 100 nm). This is in agreement with the XRD result that did not show the existence of any pure Nb phase. The reported value of Nb 3d 5/2 and Nb 3d 3/2 in  $\text{Nb}_2\text{O}_5$  is 207.5 and 210.3, respectively. From Figure 5, the position of the Nb 3d

doublet corresponds to that reported in literature for  $\text{Nb}_2\text{O}_5$ . Nb is therefore incorporated within the  $\text{TiO}_2$  lattice as  $\text{Nb}^{+5}$ . Our results are consistent with the conclusions derived by Michele et al [8] and Arbiol et al [7] in their separate studies on Nb doped  $\text{TiO}_2$  samples synthesized by sol-gel and laser induced pyrolysis, respectively. XPS study of Nb doped  $\text{TiO}_2$  samples by D. Moris et al [5] also confirm that oxidation state of Nb is  $\text{Nb}^{+5}$  for  $\text{TiO}_2$  samples doped at low Nb concentrations.



**Figure 4.** TEM bright field image of  $\text{TiO}_2$  doped with 0.5 at % Nb (a) as synthesized (b) calcined at  $500^\circ\text{C}$



**Figure 5.** High Resolution Nb 3d region for  $\text{TiO}_2$  doped with 1 at % Nb

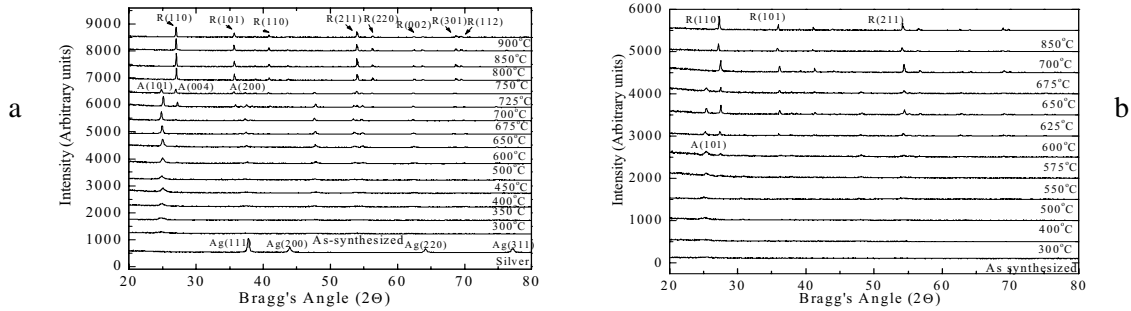


**Figure 6.** XRD Pattern as a function of calcinations temperature for  $\text{TiO}_2$  Nanoparticles doped with (a) 0.5 at % Ag (b) 1.5 at % Ag

Figures. 6a and 6b show the XRD patterns for 0.5 at % and 1.5 at % Ag doped samples, respectively. The pure silver peaks which are shown on the bottom of Figure 6a does not occur in any of the Ag-doped samples that may be attributed to the small amount of silver doping concentration. Figure 6a indicates that as synthesized and dried particles showed some degree of crystallinity in contrast to Nb doped  $\text{TiO}_2$  particles. As the annealing temperatures increased, the anatase peaks became stronger and sharper indicating improved crystallinity. Pure anatase persisted up to  $675^\circ\text{C}$ . Peaks were broad at low calcinations temperatures indicating small size nanocrystalline  $\text{TiO}_2$  particles. At  $700^\circ\text{C}$ , rutile related peaks started to appear and up to  $725^\circ\text{C}$  a mixture of both anatase and rutile phases of  $\text{TiO}_2$  were present in the sample doped with 0.5 at. % Ag. No anatase related peaks were observed at or above  $750^\circ\text{C}$  indicating a complete phase transformation from anatase to rutile. Figure 6b shows the XRD pattern obtained for  $\text{TiO}_2$  sample doped with 1.5 at. % Ag. The results indicate that at this doping concentration transformation from anatase to rutile started taking place at  $550^\circ\text{C}$  and transformation was completed at  $650^\circ\text{C}$ . Furthermore, at low temperature calcinations the anatase related peaks appeared less intensive than those appeared for samples doped with 0.5 at. % and 1.0 at. % Ag. From Figures 6a and 6b it is evident that higher contents of Ag accelerates the  $\text{TiO}_2$  anatase to rutile transformation. These results are consistent with the results of Chao et al [9]. This enhancement in the  $\text{TiO}_2$  phase transformation can be explained as below:

The atomic radii of  $\text{Ag}^{+1}$  ( $1.26 \text{ \AA}$ ) is much larger than that of  $\text{Ti}^{+4}$  ( $0.68 \text{ \AA}$ ). Due to large ionic radius, it is impossible for silver ions to act as interstitial ions in the  $\text{TiO}_2$  matrix. Therefore, the silver ion can only replace  $\text{Ti}^{+4}$  substitutionally in the lattice sites. The introduction of substitutional metal ions with valency less than 4 would induce O vacancies at the surface of anatase grains which favors

the ionic rearrangement and structure reorganization for the formation of the rutile phase [9]. The anatase to rutile phase transformation is therefore accelerated in the sample doped with 1.5 at % Ag.

Table 1 shows the average anatase grain size of the undoped and Ag-doped TiO<sub>2</sub> powders as determined by the Scherrer formula. For this purpose, anatase peak position (101) was used. It has been found that anatase grain sizes decrease in the presence of Ag dopant. With the anatase grain size decreasing, the total boundary energy for TiO<sub>2</sub> powders increases. The driving force for rutile grain growth then increases and the anatase to rutile phase transformation is promoted. Chao et al. [9] have found that corresponding to the decrease in anatase grain size specific surface area of Ag-doped TiO<sub>2</sub> powder increases. This would increase the density of surface defects at the surface of the anatase grains. The rutile nucleation is then enhanced at these surface defects. The anatase to rutile phase transformation is, therefore, promoted.

**Table 1.** Effect of Ag concentration and calcination temperature on the average anatase grain size (nm)

sample	Calcination temperature °C						
	As synthesized and dried at 60-80 °C	300	500	600	650	700	725
undoped	9	10	19	48	70	-	-
0.5 at %Ag	7	11	23	26	39	77	89
1 at % Ag	6	7	18	22	31	62	86
1.5 at % Ag	5	6	10	40*	62*	78*	88*

\* Average rutile grain sizes which are determined from the intensity of the rutile (110) peak

#### 4. Conclusions.

The presence of Nb and Ag ion doping in the TiO<sub>2</sub> nanostructure has significant effect on the transformation of anatase to rutile phase. As evident from the XRD data the mass fraction of rutile decreases by increasing the Nb content from 0.5 at. % to 1.5 at. %. Due to the comparable effective ionic radii of Ti<sup>4+</sup> and Nb<sup>5+</sup>, the lattice constants a and c of anatase relatively remained unchanged as a result of doping. XPs results indicate the incorporation of Nb as Nb<sub>2</sub>O<sub>5</sub>. Additionally, no metallic peaks were found within the XRD and XPS detection limits.

It is found that the Ag dopant accelerates the TiO<sub>2</sub> anatase to rutile transformation. This is due to an increase of oxygen vacancies at the surface of anatase grains which favors the ionic rearrangement and structure reorganization for the formation of the rutile phase [9]. The silver doping affects both the particle size and the transformation temperature. The particle size decreases with increasing doping concentration for as-synthesized samples. It varied from 9 to 5 nm.

#### 5. References

- [1] Sze Chi Chan and Mark A. Barteau, 2005 *Langmuir* **21** 5588
- [2] Andrew Burns, G.Hayes, W.Li, J.Hirvonen, J.Derek Demaree, S.Ismat Shah, 2004 *Materials Science and Engineering, BXXX MSB* **1-6** 9793
- [3] M.A.Barakat, G.Hayes and S.Ismat Shah, 2005 *J. of Nanoscience & Nanotechnology Vol.X1*
- [4] H.Z.Zhang and J.F.Banfield, 2000 *J.Phys.Chem.B* **104** 3481
- [5] D.Morris, Y.Dou, J.Rebane, C.E.J. Mitchell and R.G.Egdell, 2000 *Physical ReviewB vol. 61 No.20* 13445
- [6] U.Klueh, V.Wagner, S.Kelly, A Johnson and J.D.Bryers, 2000 *J.Biomed.Mater.Res.* **53** 621
- [7] J.Arbiol, J.Cerda, G.Dezanneau, A.Cirera, F.Peiro, A.Cornet and J.R.Mornate, 2002 *J.Apply.Phy.* **92** 853
- [8] Michele Sacerdoti, Maria Chiara Dalconi, Maria Cristina Carotta, Barbara Cavicchi, Matteo Ferroni, Stefano Colonna and Maria Luisa Di Vona 2004 *J of Solid State Chemistry* **177** 1781
- [9] H.E.Chao, Y.U.Yun, H.U.Xingfang and A.Larbot 2003 *Journal of the European Ceramic Society* **23** 1457